

Real-Time Formation of a Landau Polaron

Priya Nagpal,¹ Arnab Ghosh,¹ H el ene Seiler,² Samuel Palato,³ and Patanjali Kambhampati¹

¹*Department of Chemistry, McGill University, Montreal, H3A 0B8, Canada*

²*Freie Universit at Berlin, Arnimallee 14, 14195 Berlin, Germany*

³*Department of Chemistry, Humboldt University, Berlin 12489, Germany*

Polarons—electronic excitations dressed by a self-consistent lattice distortion—are fundamental quasiparticles in condensed-matter systems, yet their formation has not been resolved in real time. We develop a microscopic lineshape framework that connects the growth of a collective lattice polarization to the population-time evolution of the anti-diagonal linewidth in coherent multidimensional spectroscopy. Within this formalism, the anti-diagonal linewidth directly tracks the decay of lattice frequency–frequency correlations. Underdamped phonon modes yield oscillatory linewidth modulation, whereas overdamped collective polarization dynamics produce monotonic exponential broadening. Applying this criterion to multidimensional measurements on perovskite quantum dots reported in 2019, we show that the observed 150 fs exponential anti-diagonal broadening reflects the decay of a collective polarization order parameter. These results establish anti-diagonal linewidth dynamics as a direct real-time signature of Landau polaron formation.

Polarons — electronic excitations dressed by a self-consistent lattice distortion¹⁻⁴ — are fundamental quasiparticles in condensed-matter systems^{3,5-9}. Their theoretical description, originating with Landau¹ and developed through subsequent treatments of electron–phonon coupling¹⁰⁻¹², establishes that quasiparticle formation arises from the dynamical reorganization of the surrounding lattice. Yet experimental evidence has largely been limited to steady-state or long-time observables. Transport renormalization, dielectric response, and static spectral shifts reveal the presence of a dressed excitation¹³⁻¹⁷ but do not resolve the process by which the lattice distortion forms. Because lattice reorganization occurs on sub-picosecond timescales¹⁸⁻²³, most probes average over the very dynamics that define the quasiparticle.

Resolving polaron formation therefore requires a femtosecond probe that connects lattice fluctuations directly to electronic lineshapes. Coherent multidimensional spectroscopy (CMDS) provides access to homogeneous frequency–frequency correlations through the anti-diagonal (AD) linewidth of two-dimensional spectra²⁴⁻²⁶. Measurements on perovskite quantum dots revealed narrow initial homogeneous widths that broaden rapidly with population time²⁷⁻²⁹, while CdSe exhibits weak oscillatory modulation^{27,30} characteristic of underdamped phonons. These contrasting behaviors suggest fundamentally different lattice responses, but a microscopic framework linking the observed AD dynamics to Landau’s polaron picture^{1,2} has been lacking.

Here we establish that connection. Within lineshape theory,^{24-26,31} the population-time evolution of the anti-diagonal linewidth is governed directly by the decay of lattice frequency–frequency correlations. Underdamped phonon modes generate oscillatory modulation of the homogeneous linewidth, reflecting coherent lattice motion. In contrast, overdamped collective fluctuations produce monotonic growth governed by an exponential correlation decay growth arising from finite-time correlation de-

cay. The latter behavior corresponds to the dynamical formation of a Landau polaron. The resulting correlation times and scaling trends agree quantitatively with multidimensional spectroscopic measurements, identifying anti-diagonal linewidth dynamics as a direct measure of polaron formation on the timescale of atomic motion.

Figure 1 delineates the two dynamical regimes central to this work: coupling to discrete lattice normal modes and coupling to a collectively reorganizing polarization field. In crystalline semiconductors such as CdSe, lattice excitations are well-defined harmonic phonons. The time-domain Raman spectrum, obtained by Fourier transforming transient absorption oscillations, displays sharp acoustic and optical modes with minimal low-frequency spectral weight, reflecting long vibrational coherence times and weak anharmonic coupling³². In this regime, exciton–phonon interaction is well described by a displaced harmonic oscillator: photoexcitation impulsively shifts a normal-mode coordinate, generating a coherent vibrational wavepacket that oscillates reversibly about a new equilibrium. The transition frequency therefore retains phase memory on the phonon timescale, producing oscillatory modulation of the homogeneous linewidth that reflects structured lattice correlations^{27,30}.

Halide perovskites exhibit qualitatively different dynamics³³. Their vibrational spectral density is dominated by broad low-frequency weight extending to zero frequency, indicative of overdamped, diffusive lattice fluctuations rather than coherent normal modes. The relevant coordinate is not a single phonon but a collective polarization field that reorganizes following excitation^{13,27-29,34,35}. Instead of oscillatory motion, the lattice evolves toward a self-consistent distortion, and the transition frequency undergoes overdamped relaxational reorganization with exponentially decaying correlations. This overdamped regime is the dynamical setting in which a Landau polaron can form.

A number of ultrafast probes have been invoked as evi-

dence of polaron formation^{6,13,20,21,34-45}. Yet for two fundamental reasons: their observables do not project onto the relevant order parameter, and their temporal resolution is insufficient to resolve the correlation dynamics.

Transient absorption (TA) measures population changes and differential optical density^{4,13,34-36,40-42}; coherent phonons observed in TA, particularly at low temperature, reflect underdamped normal-mode oscillations rather than the overdamped buildup of a collective polarization field. Ultrafast terahertz (THz) spectroscopy measures transient photoconductivity and effective mass renormalization⁴⁴⁻⁴⁶, revealing carrier mobility and dielectric screening consistent with polaronic dressing, but it accesses transport properties rather than the decay of microscopic frequency correlations.

Angle-resolved photoemission spectroscopy (ARPES) detects band renormalization and effective mass changes⁵, and ultrafast electron or X-ray diffraction (UED) measures lattice displacement and diffuse scattering^{20,21,38,39,43}.

While these observables could in principle be related to a polaron order parameter, no framework has connected them to the decay of correlation functions that govern quasiparticle formation. Moreover, typical instrument response functions exceeding 100 fs are insufficient to resolve the 150 fs correlation time characteristic of polaron formation. Quantitative observation further requires near-band-edge excitation at low fluence to avoid hot-carrier and multiparticle effects that obscure intrinsic lattice reorganization. As a result, the decay of frequency memory that defines polaron birth has remained experimentally inaccessible until recently²⁷⁻²⁹.

Coherent multidimensional spectroscopy uniquely resolves the anti-diagonal (AD) linewidth, which directly reflects frequency–frequency correlations during the population time^{24-26,47}. In perovskite quantum dots, the AD linewidth evolves from an initially narrow homogeneous width to exponential broadening with systematic halide and size dependence²⁷⁻²⁹, whereas CdSe exhibits weak oscillatory modulation^{27,30}. These contrasting behaviors point to distinct lattice responses. What has been lacking is a microscopic framework connecting this observable to Landau’s description of polaron formation. Establishing that connection is the objective of the theory developed below.

We now develop the microscopic framework linking lattice dynamics to the measured anti-diagonal (AD) linewidth. Within the Kubo–Anderson formalism, the population-time evolution of the AD linewidth is governed directly by the frequency–frequency correlation function $C_\omega(t)$ of the transition energy^{24-26,31}. Underdamped phonon environments produce oscillatory, sign-changing correlations that manifest as reversible modulation of the homogeneous linewidth^{27,30}. In contrast, overdamped collective fluctuations lead to monotonic exponential decay of frequency correlations and cor-

responding monotonic linewidth growth²⁷⁻²⁹. It is this overdamped correlation decay that characterizes the dynamical formation of a Landau polaron.

Polaron formation is the time-dependent emergence of a collective lattice polarization surrounding an electronic excitation^{1,2,5}. An exciton generates a local electric field $E_{exc}(\mathbf{r})$ that couples to the lattice polarization density $P(\mathbf{r}, t)$, shifting the transition energy according to

$$\delta E(t) = - \int d^3r P(\mathbf{r}, t) \cdot E_{exc}(\mathbf{r}). \quad (1)$$

Because the distortion involves many lattice degrees of freedom, we introduce a coarse-grained scalar order parameter $\eta(t)$, defined as the polarization projected along the excitonic field and averaged over the polaron volume V_{pol} ,

$$\eta(t) = \frac{1}{V_{pol}} \int_{V_{pol}} d^3r \hat{e} \cdot P(\mathbf{r}, t). \quad (2)$$

This coordinate is not a normal phonon mode and, at room temperature, is generically overdamped. Substituting Eq. (2) into Eq. (1) yields a linear coupling between the order parameter and the transition frequency,

$$\delta\omega(t) = g\eta(t), \quad (3)$$

where g is an effective exciton–lattice coupling constant. The experimentally relevant quantity is the correlation function of these fluctuations,

$$C_\omega(t) = \langle \delta\omega(t)\delta\omega(0) \rangle = g^2 \langle \delta\eta(t)\delta\eta(0) \rangle. \quad (4)$$

Linearizing fluctuations about the mean polarization yields relaxational dynamics of a coarse-grained order parameter. Near equilibrium, such overdamped Langevin dynamics reduce generically to a linear stochastic equation whose stationary solution is the Ornstein–Uhlenbeck process⁴⁸,

$$\frac{d\delta\eta(t)}{dt} = -\frac{1}{\tau_{pol}}\delta\eta(t) + \xi(t), \quad (5)$$

with $\langle \xi(t) \rangle = 0$ and $\langle \xi(t)\xi(0) \rangle \propto \delta(t)$, corresponding to Gaussian white-noise driving of the overdamped order parameter. The resulting correlation function is

$$\langle \delta\eta(t)\delta\eta(0) \rangle = \langle \delta\eta^2 \rangle e^{-|t|/\tau_{pol}}. \quad (6)$$

Within second-order cumulant theory³¹, the optical coherence decay is determined by

$$g(t) = \int_0^t d\tau \int_0^\tau d\tau' C_\omega(\tau'), \quad (7)$$

and in two-dimensional spectroscopy the anti-diagonal linewidth isolates this homogeneous contribution. For exponential correlations, the AD width evolves as

$$\Gamma_{AD}(t_2) \approx \Gamma_\infty \sqrt{1 - e^{-t_2/\tau_p}}. \quad (8)$$

Equation (8) follows from the Ornstein–Uhlenbeck description of frequency fluctuations, in which the frequency variance evolves as $1 - e^{-t_2/\tau_p}$. Because the anti-diagonal linewidth is proportional to the square root of this variance, the linewidth itself follows the square-root dependence given above. This expression represents the minimal result for an Ornstein–Uhlenbeck frequency-fluctuation process in the experimentally relevant limit where static inhomogeneous broadening exceeds the initial homogeneous linewidth^{31,49–51}. More complete treatments show that the absolute anti-diagonal linewidth at $t_2 = 0$ depends on the full set of homogeneous and inhomogeneous broadening parameters and may exhibit weak deviations from strictly monotonic behavior as the static limit is approached. However, the characteristic growth time extracted from the linewidth evolution remains equal to the correlation time τ_p , which is the primary quantity of interest here.

Equation (8) therefore establishes the central result of this work: the population-time evolution of the anti-diagonal linewidth directly measures the decay of the order-parameter correlation function associated with collective lattice polarization. Monotonic growth of the linewidth is the dynamical signature of overdamped relaxational polarization dynamics, whereas underdamped phonons produce primarily oscillatory modulation without cumulative spectral diffusion. Because the anti-diagonal linewidth isolates homogeneous frequency–frequency correlations, the observation of monotonic linewidth growth implies a finite-time decay of a collective polarization field. The multidimensional measurements reported in 2019²⁷ exhibit precisely this behavior on a 150 fs timescale, thereby satisfying the theoretical criterion for resolving Landau-polaron formation in real time. The population-time evolution of the anti-diagonal linewidth is thus naturally described by an Ornstein–Uhlenbeck frequency-fluctuation process, providing a minimal stochastic representation of order-parameter formation in a photoexcited polar quantum material.

Figure 2 illustrates the stochastic dynamics implied by the overdamped order-parameter model. For exponential correlation decay with characteristic time τ_{pol} , the transition frequency exhibits colored noise with finite memory. Fig2a shows representative growth of the lattice order parameter following excitation, highlighting the emergence of a well-defined reorganization time. Fig2b presents sample trajectories generated by the Ornstein–Uhlenbeck process, demonstrating bounded stochastic fluctuations rather than coherent oscillations. Fig2c displays the corresponding autocorrelation functions, which converge to the exponential form $C(t) = e^{-t/\tau_{pol}}$. Within cumulant theory³¹, this decay directly produces the monotonic evolution of the anti-diagonal linewidth predicted by Eq. (8).

Figure 3 connects these stochastic correlations to multidimensional spectroscopy. Fig3a shows the CMDS

pulse sequence, in which frequency correlations accumulated during the population time t_2 determine the anti-diagonal width of the two-dimensional spectrum. Fig3b presents calculated spectra at early and late t_2 : initially elongated along the diagonal when frequency memory is preserved, and progressively circular as memory decays. This lineshape evolution reflects spectral diffusion governed by $C(t_2)$. Fig3c compares correlation functions for perovskite and CdSe quantum dots. Perovskites exhibit monotonic exponential decay consistent with overdamped collective dynamics, whereas CdSe displays weak decay with oscillatory structure characteristic of coherent LO phonons. The corresponding linewidth dynamics, computed from Eq. (8) and compared with experiment, reproduce the exponential broadening observed in perovskites and the oscillatory modulation seen in CdSe.

The coherent multidimensional measurements therefore resolve the decay of frequency correlations in real time. In perovskite quantum dots, the observed exponential anti-diagonal broadening signifies overdamped collective polarization dynamics, while CdSe remains in the underdamped phonon regime. The linewidth evolution thus reflects the emergence of a lattice distortion surrounding the exciton and provides direct access to the real-time formation of a Landau polaron.

In conclusion, the formation of a Landau polaron—the dynamical dressing of an electronic excitation by a self-consistent lattice distortion—has long been inferred from steady-state renormalization effects but not resolved in time. Conventional probes reveal transport renormalization, dielectric screening, or structural displacement, yet they do not isolate the decay of frequency correlations that governs quasiparticle emergence. Here we establish that the waiting-time evolution of the anti-diagonal linewidth in coherent multidimensional spectroscopy directly reflects the correlation function of a collective lattice polarization order parameter. Within this framework, monotonic growth governed by an exponential correlation decay growth is the necessary dynamical consequence of overdamped polarization-field relaxation. Because the multidimensional measurements reported in 2019 exhibit precisely this exponential correlation decay on a 150 fs timescale, the observed anti-diagonal linewidth evolution constitutes a direct real-time observation of Landau polaron formation.

Supplementary Information. Details of the theory and fitting are provided in the SI.

Acknowledgements. Financial support from NSERC and McGill University is acknowledged.

-
- [1] L. Landau and S. Pekar, Zh. Eksp. Teor. Fiz **18**, 419 (1948).
 - [2] L. D. Landau, Phys. Z. Sowjet. **3**, 664 (1933).

- [3] J. Lafuente-Bartolome, C. Lian, W. H. Sio, I. G. Gurtubay, A. Eiguren, and F. Giustino, *Phys. Rev. Lett.* **129**, 076402 (2022).
- [4] C. D. Sonnichsen, D. P. Strandell, P. J. Brosseau, and P. Kambhampati, *Phys. Rev. Research* **3**, 023147 (2021).
- [5] C. Franchini, M. Reticcioli, M. Setvin, and U. Diebold, *Nat. Rev. Mater.* **6**, 560 (2021).
- [6] A. Vashisht, I. Amelio, L. Vanderstraeten, G. M. Bruun, O. K. Diessel, and N. Goldman, *Nat. Commun.* **16**, 4918 (2025).
- [7] A. Geondzhian, A. Sambri, G. M. De Luca, R. Di Capua, E. Di Gennaro, D. Betto, M. Rossi, Y. Y. Peng, R. Fumagalli, and N. B. Brookes, *Phys. Rev. Lett.* **125**, 126401 (2020).
- [8] Z. Dai, C. Lian, J. Lafuente-Bartolome, and F. Giustino, *Phys. Rev. B* **109**, 045202 (2024).
- [9] W. H. Sio, C. Verdi, S. Ponc e, and F. Giustino, *Phys. Rev. Lett.* **122**, 246403 (2019).
- [10] S. Pekar, *Local quantum states of electrons in an ideal ion crystal* (1946) *zhurnal Eksperimentalnoi i Teoreticheskoi Fiziki* **16**, 341–348 (1946).
- [11] H. Fr ohlich, *Adv. Phys.* **3**, 325 (1954).
- [12] R. P. Feynman, *Phys. Rev.* **97**, 660 (1955).
- [13] K. Miyata, D. Meggiolaro, M. T. Trinh, P. P. Joshi, E. Mosconi, S. C. Jones, F. De Angelis, and X. Y. Zhu, *Sci. Adv.* **3**, e1701217 (2017).
- [14] D. Bao, Q. Chang, B. Chen, X. Chen, H. Sun, Y. M. Lam, D. Zhao, J.-X. Zhu, and E. E. Chia, *PRX Energy* **2**, 013001 (2023).
- [15] M. Puppini, S. Polishchuk, N. Colonna, A. Crepaldi, D. N. Dirin, O. Nazarenko, R. De Gennaro, G. Gatti, S. Roth, T. Barillot, L. Poletto, R. P. Xian, L. Rettig, M. Wolf, R. Ernstorfer, M. V. Kovalenko, N. Marzari, M. Grioni, and M. Chergui, *Phys. Rev. Lett.* **124**, 206402 (2020).
- [16] J. M. Frost, *Phys. Rev. B* **96**, 195202 (2017).
- [17] M. J. Schilcher, P. J. Robinson, D. J. Abramovitch, L. Z. Tan, A. M. Rappe, D. R. Reichman, and D. A. Egger, *ACS Energy Lett.* **6**, 2162 (2021).
- [18] D. Filippetto, P. Musumeci, R. Li, B. J. Siwick, M. Otto, M. Centurion, and J. Nunes, *Rev. Mod. Phys.* **94**, 045004 (2022).
- [19] V. R. Morrison, R. P. Chatelain, K. L. Tiwari, A. Hendaoui, A. Bruh acs, M. Chaker, and B. J. Siwick, *Science* **346**, 445 (2014).
- [20] B. Guzelturk, T. Winkler, T. W. J. Van de Goor, M. D. Smith, S. A. Bourelle, S. Feldmann, M. Trigo, S. W. Teitelbaum, H. G. Steinr uck, G. A. de la Pena, R. Alonso-Mori, D. Zhu, T. Sato, H. I. Karunadasa, M. F. Toney, F. Deschler, and A. M. Lindenberg, *Nat. Mater.* **20**, 618 (2021).
- [21] X. X. Wu, L. Z. Tan, X. Z. Shen, T. Hu, K. Miyata, M. T. Trinh, R. K. Li, R. Coffee, S. Liu, D. A. Egger, I. Makasyuk, Q. Zheng, A. Fry, J. S. Robinson, M. D. Smith, B. Guzelturk, H. I. Karunadasa, X. J. Wang, X. Y. Zhu, L. Kronik, A. M. Rappe, and A. M. Lindenberg, *Sci. Adv.* **3**, e1602388 (2017).
- [22] G. Sciaini and R. D. Miller, *Rep. Prog. Phys.* **74**, 096101 (2011).
- [23] B. J. Siwick, J. R. Dwyer, R. E. Jordan, and R. D. Miller, *Science* **302**, 1382 (2003).
- [24] S. Biswas, J. Kim, X. Zhang, and G. D. Scholes, *Chem. Rev.* **122**, 4257 (2022).
- [25] E. Fresch, F. V. Camargo, Q. Shen, C. C. Bellora, T. P ullerits, G. S. Engel, G. Cerullo, and E. Collini, *Nat. Rev. Methods Primers* **3**, 84 (2023).
- [26] D. M. Jonas, *Annu. Rev. Phys. Chem.* **54**, 425 (2003).
- [27] H. Seiler, S. Palato, C. Sonnichsen, H. Baker, E. Socie, D. P. Strandell, and P. Kambhampati, *Nat. Commun.* **10**, 4962 (2019).
- [28] P. Brosseau, A. Ghosh, H. Seiler, D. Strandell, and P. Kambhampati, *J. Chem. Phys.* **159** (2023).
- [29] A. Ghosh, S. Palato, P. Brosseau, R. Tao, D. N. Dirin, M. V. Kovalenko, and P. Kambhampati, *ACS Nano* **19**, 26843 (2025).
- [30] H. Seiler, S. Palato, and P. Kambhampati, *J. Chem. Phys.* **149**, 074702 (2018).
- [31] S. Mukamel, *Principles of Nonlinear Optical Spectroscopy* (Oxford University Press, 1995).
- [32] D. M. Sagar, R. R. Cooney, S. L. Sewall, E. A. Dias, M. M. Barsan, I. S. Butler, and P. Kambhampati, *Phys. Rev. B* **77**, 235321 (2008).
- [33] A. Ghosh, A. Liu, S. C. Boehme, P. Brosseau, D. N. Dirin, M. V. Kovalenko, and P. Kambhampati, *ACS Nano* **19**, 19927 (2025).
- [34] K. Miyata, T. L. Atallah, and X. Y. Zhu, *Sci. Adv.* **3**, e1701469 (2017).
- [35] F. Thouin, D. A. Valverde-Ch avez, C. Quarti, D. Cortecchia, I. Bargigia, D. Beljonne, A. Petrozza, C. Silva, and A. R. Srimath Kandada, *Nat. Mater.* **18**, 349 (2019).
- [36] S. Biswas, R. Zhao, F. Alowa, M. Zacharias, S. Sharifzadeh, D. F. Coker, D. S. Seferos, and G. D. Scholes, *Nat. Mater.* (2024).
- [37] S. A. Bretschneider, I. Ivanov, H. I. Wang, K. Miyata, X. Y. Zhu, and M. Bonn, *Adv. Mater.* **30**, 1707312 (2018).
- [38] H. Seiler, D. Zahn, V. C. Taylor, M. I. Bodnarchuk, Y. W. Windsor, M. V. Kovalenko, and R. Ernstorfer, *ACS Nano* **17**, 1979 (2023).
- [39] S. A. Cuthriell, S. Panuganti, C. C. Laing, M. A. Quintero, B. Guzelturk, N. Yazdani, B. Traore, A. Brumberg, C. D. Malliakas, and A. M. Lindenberg, *Adv. Mater.* **34**, 2202709 (2022).
- [40] G. Batignani, G. Fumero, A. R. Srimath Kandada, G. Cerullo, M. Gandini, C. Ferrante, A. Petrozza, and T. Scopigno, *Nat. Commun.* **9**, 1971 (2018).
- [41] M. Park, A. J. Neukirch, S. E. Reyes-Lillo, M. Lai, S. R. Ellis, D. Dietze, J. B. Neaton, P. Yang, S. Tretiak, and R. A. Mathies, *Nat. Commun.* **9**, 2525 (2018).
- [42] T. Debnath, D. Sarker, H. Huang, Z.-K. Han, A. Dey, L. Polavarapu, S. V. Levchenko, and J. Feldmann, *Nat. Commun.* **12**, 2629 (2021).
- [43] T. L. Britt, F. Caruso, and B. J. Siwick, *npj Comput. Mater.* **10**, 178 (2024).
- [44] Y. Lan, B. J. Dringoli, D. A. Valverde-Chavez, C. S. Ponceca, M. Sutton, Y. H. He, M. G. Kanatzidis, and D. G. Cooke, *Sci. Adv.* **5**, eaaw5558 (2019).
- [45] X. Yue, C. Wang, B. Zhang, Z. Zhang, Z. Xiong, X. Zu, Z. Liu, Z. Hu, G. O. Odunmbaku, and Y. Zheng, *Nat. Commun.* **14**, 917 (2023).
- [46] E. Cinquanta, D. Meggiolaro, S. G. Motti, M. Gandini, M. J. P. Alcocer, Q. A. Akkerman, C. Vozzi, L. Manna, F. De Angelis, and A. Petrozza, *Phys. Rev. Lett.* **122**, 166601 (2019).
- [47] M. K. Petti, J. P. Lomont, M. Maj, and M. T. Zanni, *J. Phys. Chem. B* **122**, 1771 (2018).
- [48] T. Uneyama, T. Miyaguchi, and T. Akimoto, *Phys. Rev. E* **99**, 032127 (2019).
- [49] R. Kubo, *J. Phys. Soc. Jpn.* **9**, 935 (1954).

- [50] M. Zanni and P. Hamm, *Concepts and Methods of 2D Infrared Spectroscopy* (Cambridge University Press, 2011).
- [51] H. Li, B. Lomsadze, G. Moody, C. Smallwood, and S. Cundiff, *Optical Multidimensional Coherent Spectroscopy* (Oxford University Press, 2023).

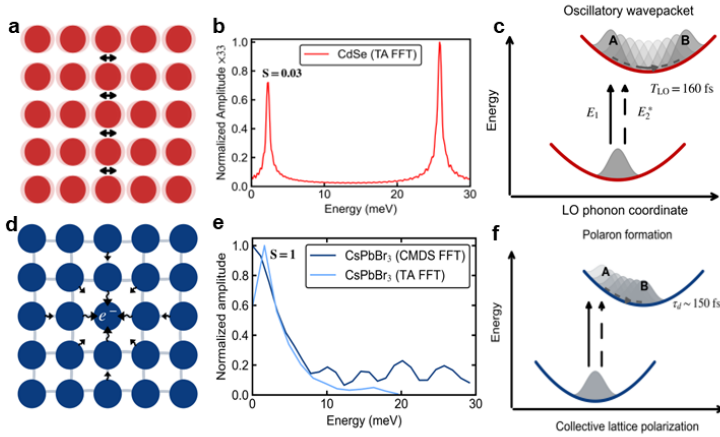


FIG. 1. Distinction between normal-mode phonons and collective polarization dynamics. (a) In crystalline semiconductors such as CdSe, lattice excitations are well-defined normal modes. (b) Time-domain Raman spectrum of CdSe quantum dots obtained by Fourier transforming transient absorption oscillations, showing sharp acoustic and optical phonons with negligible low-frequency spectral weight. (c) Displaced harmonic oscillator model illustrating coherent phonon dressing: excitation impulsively shifts a normal-mode coordinate, producing reversible oscillatory modulation of the transition energy. (d) In halide perovskites, lattice response is dominated by dynamically soft, anharmonic fluctuations rather than discrete modes. (e) Corresponding spectral density extracted from CMDS and transient absorption exhibits broad low-frequency weight extending to zero frequency, indicative of overdamped fluctuations. (f) Configuration coordinate for a collective polarization field: following excitation, the lattice evolves diffusively toward a self-consistent distortion rather than oscillating coherently. This overdamped regime enables Landau polaron formation.

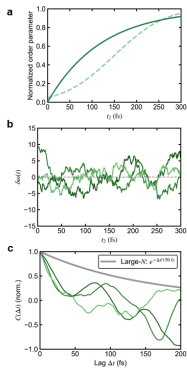


FIG. 2. Stochastic dynamics of an overdamped lattice order parameter. (a) Representative time evolution of a normalized lattice order parameter following excitation, illustrating a characteristic reorganization time, following solution of Eq. (5). (b) Sample stochastic trajectories of transition-frequency fluctuations generated by an Ornstein–Uhlenbeck process with correlation time τ_{pol} . (c) Autocorrelation functions of the trajectories in (b), converging to exponential decay $C(t) = \exp(-t/\tau_{\text{pol}})$. Exponential memory loss of the order parameter produces monotonic anti-diagonal linewidth growth within cumulant lineshape theory.

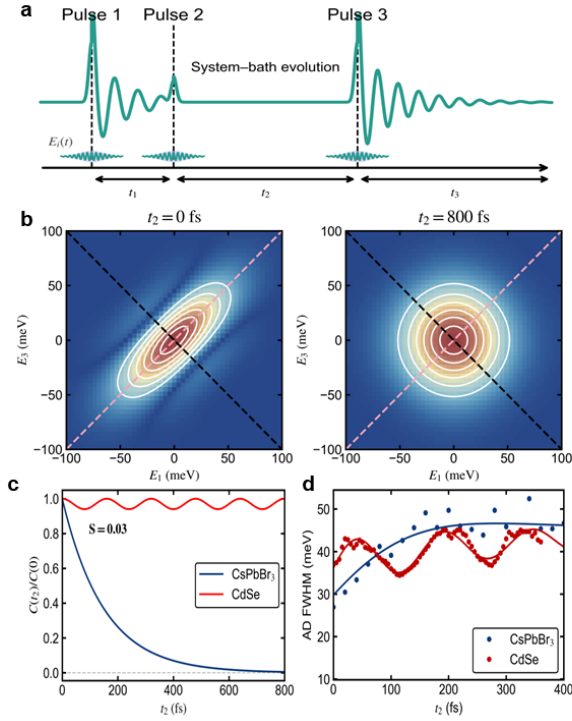


FIG. 3. Connection between correlation decay and multidimensional lineshape evolution. (a) CMDS pulse sequence consisting of three phase-resolved electric fields shown above the time axis. The first pulse creates a coherence, the second converts it to a population that evolves during waiting time t_2 under system–bath interactions, and the third converts the evolved state into a radiated third-order polarization. Frequency correlations accumulated during t_2 determine the anti-diagonal linewidth. (b) Calculated two-dimensional spectra at early and late t_2 . Initially, excitation and emission frequencies are correlated, producing a diagonally elongated spectrum with narrow anti-diagonal width. As correlations decay, the spectrum becomes more circular and the anti-diagonal width increases, reflecting spectral diffusion governed by $C(t_2)$. (c) Measured and modeled frequency–frequency correlation functions for perovskite and CdSe quantum dots. Perovskites exhibit monotonic exponential decay consistent with overdamped collective polarization dynamics, whereas CdSe shows weak decay with oscillatory structure characteristic of coherent LO phonons. (d) Population-time evolution of the anti-diagonal linewidth. The solid curves are calculated from Eq. (8) using the correlation functions in panel (c), and symbols represent experimental measurements. Perovskites exhibit monotonic linewidth growth governed by exponential correlation decay, whereas CdSe shows oscillatory modulation without cumulative broadening. The agreement demonstrates that the observed linewidth dynamics directly reflect the underlying correlation functions and constitute a real-time signature of Landau polaron formation.